THERMO-MECHANICAL COUPLING ANALYSIS AND SOFTWARE DEVELOPMENT

by

Jianwei CHAI**, *Hua AI, and Ting LIU

Langfang Yanjing Vocational Technology College, China

Original scientific paper
https://doi.org/10.2298/TSCI2104199C

In order to quickly and accurately grasp the law of freeze-thaw reaction of permafrost slopes, based on the hydro-thermal-mechanical coupling theory, relying on MATLAB to compile a finite element program that can reflect the multi-field coupling mechanism of the soil. This test is in good agreement with the classic test, which verifies the reliability of the program. Based on this, the paper developed a set of water-thermal-mechanical coupling analysis software for permafrost slopes that can run independently and is easy to operate. The software's functions and development process are introduced. The response characteristics of frozen soil slopes under freezing and thawing are analyzed in combination with the example papers. The results show that the slope temperature, moisture, stress and displacement are obviously different at different times. The maximum shear stress band appears at the freezing-thawing interface of the slope. The horizontal displacement of the slope is basically the same along the slope when the freezing is completed. At the end of the thawing period, the upper part and the lower part are large. The horizontal displacement and unfrozen water content of the slope during the thawing period are larger than those during the freezing period, but the maximum shear stress is small and the stability of permafrost in the warm season is poor. It has important application value for freeze-thaw calculation of frozen soil slope engineering.

Key words: *numerical calculation, software development, permafrost slope, hydro-thermal-mechanical coupling, freezing and thawing*

Introduction

Permafrost occupies 21.5% of my country's land area. In recent years, large-scale earth excavation and filling works have been carried out in frozen soil areas. Disturbance to the geological environment has made many frozen soil slopes unstable. For example, a thawing mudflow landslide occurs near section K3057 of the Qinghai-Tibet highway, the landslide body of section K3035 retreats to the top of the mountain by about 100 m within five years, and the mudflow landslide moves toward the Qinghai-Tibet highway, which will affect the normal operation of the highway. Some scholars classify the failure of permafrost slopes on the Qinghai-Tibet Plateau as: collapse, creep, thermal thawing instability, and mud flow. Frontiers and others classified the main types and characteristics of freezing damage in permafrost regions, and proposed prevention and control measures [1]. Some scholars analyzed the failure mechanism of rock and soil slopes in cold areas, and gave the corresponding stability calculation methods. Some scholars have conducted experimental research on soil slope freeze-thaw insta-

* Corresponding author, e-mail: jianweichai2991@163.com

bility and vegetation slope protection in cold regions. Monitoring shows that during the freezing process of slopes, water migrates to the freezing front, and woody plant slope protection helps reduce slope freeze-thaw instability. Some scholars discussed the failure mechanism of low angle frozen soil slopes, conducted freeze-thaw model tests, and gave the stability analysis methods of frozen soil slopes under different seepage conditions.

Based on the three-field coupling theory of water, heat and force, this paper compiled a multi-field coupling calculation program that can reflect soil frost heave and thaw settlement, developed a hydro-thermal-mechanical coupling analysis software for frozen soil slopes, and established a multi-field coupled calculation model for permafrost slopes. Analyzed the temperature, moisture, stress and deformation distribution law of the slope during freezing and thawing, and provided convenience and reference for the engineering calculation of frozen soil slope.

The coupled hydro-thermal-mechanical control equation of frozen soil slope

Under the action of periodic freeze-thaw cycles, the heat conduction between the frozen soil skeleton and water and the ice-water phase transition, the temperature in the frozen soil slope satisfies the heat conduction equation of the transient temperature field with phase change:

$$C\frac{\partial T}{\partial t}=\frac{\partial}{\partial x}\left(\lambda\frac{\partial T}{\partial x}\right)+\frac{\partial}{\partial y}\left(\lambda\frac{\partial T}{\partial y}\right)+L\rho_i\frac{\partial\theta_i}{\partial t} \tag{1}$$

where C is the volumetric specific heat capacity, T – the temperature, t – the time, x and y – the co-ordinate system, λ – the thermal conductivity, L – the latent heat of phase change, ρ_i – the density of ice, and θ_i – the volume content of ice [2]. Under the action of freezing and thawing, the water migration in the frozen soil slope is carried out by liquid water, then the water migration equation:

$$\frac{\partial\theta_u}{\partial t}=\frac{\partial}{\partial x}\left(D\frac{\partial\theta_u}{\partial x}\right)+\frac{\partial}{\partial y}\left(D\frac{\partial\theta_u}{\partial y}\right)+\frac{\rho_i}{\rho_w}\frac{\partial\theta_i}{\partial t} \tag{2}$$

where θ_u is the volume content of unfrozen water, D – the water diffusion coefficient, and ρ_w – the density of water. The relationship between the unfrozen water content and temperature of frozen soil:

$$\theta_u=\begin{cases} a\left|T\right|^{-b} & T<0 \\ \theta_w & T\geq 0 \end{cases} \tag{3}$$

where a and b are the parameters related to the properties of the soil, respectively, and θ_w – the total water content. The paper substitutes eq. (1) into eq. (2), and simplifies the derived relationship of eq. (3) to obtain the hydrothermal coupling equation:

$$C^*\frac{\partial T}{\partial t}=\frac{\partial}{\partial x}\left(\lambda^*\frac{\partial T}{\partial x}\right)+\frac{\partial}{\partial y}\left(\lambda^*\frac{\partial T}{\partial y}\right) \tag{4}$$

where

$$C^*=C+L\rho_w\frac{\partial\theta_u}{\partial t},\ \ \lambda^*=\lambda+L\rho_w\frac{\partial\theta_u}{\partial t}$$

paper adopts the sensible heat capacity method to consider the phase change surface. Assuming that the phase change of the soil occurs in a temperature range ($T_m+\Delta T$) near T_m, the simplified structure of the volume heat capacity and thermal conductivity expression:

$$C = \begin{cases} C_f & T < T_m - \Delta T \\ \dfrac{C_f + C_u}{2} & T_m - \Delta T \le T \le T_m - \Delta T \\ C_u & T > T_m + \Delta T \end{cases} \tag{5}$$

$$\lambda = \begin{cases} \lambda_f & T < T_m - \Delta T \\ \lambda_f \dfrac{\lambda_u - \lambda_f}{2\Delta T} & \left[T - \left(T_m - \Delta T\right)\right] \\ \lambda_u & T > T_m + \Delta T \end{cases} \tag{6}$$

where C_f is the specific heat capacity of frozen soil, λ_f – the thermal conductivity of frozen soil, C_u – the specific heat capacity of melting soil, λ_u – the thermal conductivity of melting soil, T_m – the midpoint temperature of the phase transition interval, and ΔT – the midpoint temperature of the phase transition interval and the highest or lowest the absolute difference in phase transition temperature [3]. The static balance differential equation of frozen soil slope:

$$[\partial]\{\sigma\} - \{f\} = 0 \tag{7}$$

The physical equation:

$$\{\sigma\} = [D_r]\left(\{\varepsilon\} - \{\varepsilon^\upsilon\}\right) \tag{8}$$

The geometric equation:

$$\{\varepsilon\} = [\partial]^T \{u\} \tag{9}$$

where $[\partial]$ is the matrix differential operator, $\{\sigma\}$ – the stress, $\{f\}$ – the physical force, $[D_r]$ – the temperature-related elastic matrix, E – the elastic strain, $\{\varepsilon^\upsilon\}$ – the strain caused by frost heave or melting, and $\{u\}$ – the displacement. Among them:

$$[\partial] = \begin{bmatrix} \dfrac{\partial}{\partial x} & 0 & \dfrac{\partial}{\partial y} \\ 0 & \dfrac{\partial}{\partial y} & \dfrac{\partial}{\partial x} \end{bmatrix}, \quad [D_r] = \frac{E}{(1+\mu)(1+2\mu)} \begin{bmatrix} 1-\mu & \mu & 0 \\ \mu & 1-\mu & 0 \\ 0 & 0 & \dfrac{(1-2\mu)}{2} \end{bmatrix}$$

$$E = a_1 + b_1 |T|^m, \ \mu = a_2 + b_2 |T|, \ \{\varepsilon^\upsilon\} = \{\varepsilon_x^\upsilon \varepsilon_y^\upsilon \varepsilon_{xy}^\upsilon\}$$

when freezing

$$\varepsilon_x^\upsilon = \varepsilon_y^\upsilon = \frac{1}{3}\left\{1.09\left(\theta_0 + \Delta\theta - \theta_u\right) + \left(\theta_u - n\right)\right\}, \ \gamma_{xy}^\upsilon = 0$$

when melting

$$\varepsilon_x^\upsilon = \varepsilon_y^\upsilon = \frac{1}{3} A, \ \gamma_{xy}^\upsilon = 0$$

where E is the modulus of elasticity, μ – the Poisson's ratio, $\Delta\theta$ – the amount of water migration in a certain period of time, n – the porosity of the soil, A – the thawing coefficient, a_1, b_1, a_2, b_2, and m – the parameter related to soil properties, respectively. Equations (1)-(9) constitute the coupled hydro-thermal-mechanical equations of permafrost slopes. Because soil thermodynamic parameters change with temperature, and there is a time-varying freeze-thaw interface in the calculation model area, the freeze-thaw interface produces phase changes, so the previous equation describes a strong non-linearity with a large space and large time scale [4]. The problem cannot be solved analytically, so the numerical method is used to solve the problem. In this paper, the control equation of frozen soil slope is discretized in the space domain by finite element, and the time domain is discretized by finite difference. The two are combined and iteratively solved. Multi-field coupling calculation software for soil slopes.

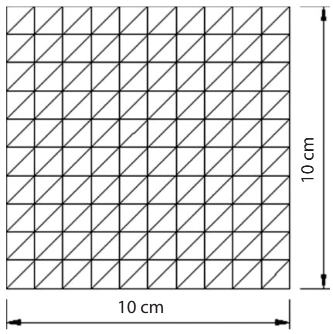

Figure 1. Finite element numerical analysis model of PENNER experimental specimen

Program verification and software development

Documentary program verification

In order to verify the correctness of the hydro-thermal-mechanical coupling program, the paper uses PENNER to study the frozen soil ice lens formation process experiment and MU and other numerical calculations of the experiment to verify the correctness of the hydro-thermal-mechanical coupling program in this paper. The thermal, mechanical parameters and boundary conditions of the soil are the same as those in the literature, tab. 1. The analysis model is shown in fig. 1, and the temperature boundary is shown in fig. 2. Using the developed program to calculate, select freezing depth and frost heave amount for comparative analysis, the results are shown in figs. 3 and 4.

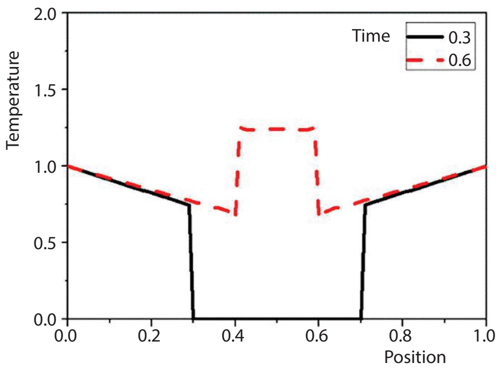

Figure 2. Temperature boundary conditions

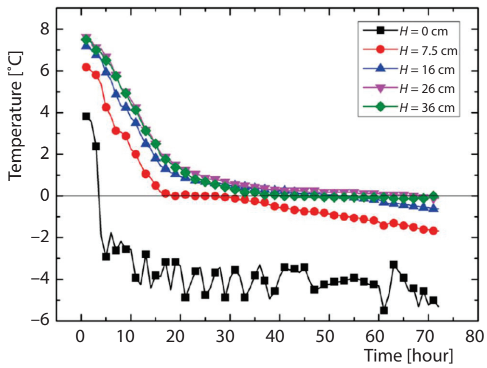

Figure 3. The curve of freezing depth *vs.* time

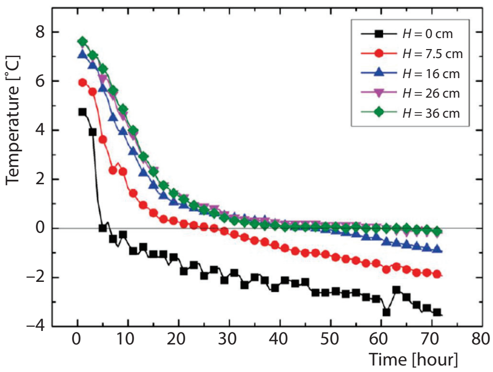

Figure 4. Curve of frost heave over time

The water content of the test soil is 0.35, and the functional relationship between unfrozen water and negative soil temperature:

$$n_w = \begin{cases} 0.35 & T \geq -0.11\ ^\circ\text{C} \\ 0.104109(-T)^{-0.5564} & T < -0.11\ ^\circ\text{C} \end{cases} \tag{10}$$

Frozen soil is regarded as a linear elastic body, and the Poisson's ratio of frozen soil and unfrozen soil is both 0.3. The elastic model when not frozen is 11.2 MPa, and the elastic modulus when frozen:

$$E_0 = 4 \cdot 10^2 |T|^{0.636} \tag{11}$$

Table 1. Thermodynamic parameters of model soil

Ingredient	Soil parameters	
	Heat capacity [°CJm^{-3}k^{-1}]	Thermal conductivity, λ [Wm^{-1}k^{-1}]
Water	$4.18 \cdot 10^6$	0.602
Ice	$1.93 \cdot 10^6$	2.22
Soil particles	$2.2 \cdot 10^6$	1.95

Horiguchi experiment results for soil hydraulic conductivity:

$$k = \begin{cases} 3.072 \cdot 10^{-11} \mathrm{e}^{13.438T} & T > -0.3 \ ^\circ\mathrm{C} \\ 3.453 \cdot 10^{-13} & T \leq -0.3 \ ^\circ\mathrm{C} \end{cases} \tag{12}$$

Initial temperature and boundary conditions: The top of the soil is the warm end, the bottom is the cold end, and freezing from bottom to top. The boundary conditions are shown in fig. 2. In order to simulate the initial state of the sample before freezing, the paper takes the upper and lower boundary temperatures at $t = 0$ as the initial temperature, and solves the Laplace equation using the initial temperature conditions and the thermal parameters of the soil and other characteristic parameters to obtain the temperature of the calculated area. The estimated value of the field, after correcting the parameters, continue to calculate until the stable temperature field is used as the initial temperature field.

Moisture boundary conditions: The soil body is saturated soil and water is recharged from the bottom boundary (from the warm end) when frozen. Displacement boundary conditions: the bottom of the soil is constrained, the left and right sides are normal constraints, and the top is the free displacement boundary [5]. It can be seen from figs. 3 and 4 that the freezing depth obtained at different moments is slightly smaller than the experimental value, and is closer to the experimental value than the MU calculation result; the frost heave at each moment is slightly smaller than the experimental value, and the first half of the calculation is less than the MU calculation. It can be concluded that the change law of freezing depth and frost heave amount obtained in this paper is consistent with the law of PENNER experimental MU analysis results, and the values are similar, indicating that the compiled program is reliable and effective.

Software development

Relying on the MATLAB platform and based on the theory of hydro-thermal-mechanical coupling, the dissertation has developed an independent, object-oriented, interface-friendly and easy-to-operate hydro-thermal-mechanical coupling analysis software for permafrost slopes [6]. The software includes a pre-processor (model size, input of soil physical parameters and meshing), a solver (iterative solution) and a post-processor (result storage and cloud map display). The development flow chart is shown in fig. 5. The software the main interface, model generation, parameter input and calculation result display interface are shown in figs. 6 and 7. The software can efficiently and accurately calculate the temperature, moisture, stress and displacement of permafrost slopes under the action of external temperature, and has important theoretical significance and application value for the calculation of frozen soil slopes.

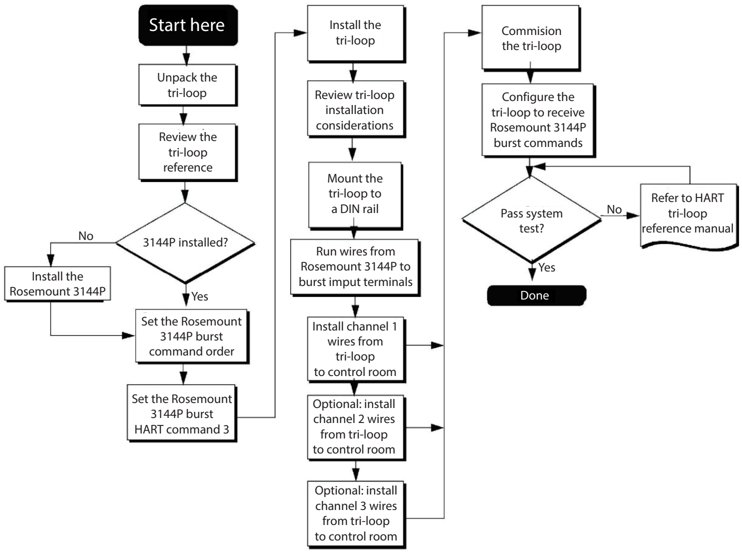

Figure 5. Software program design block diagram

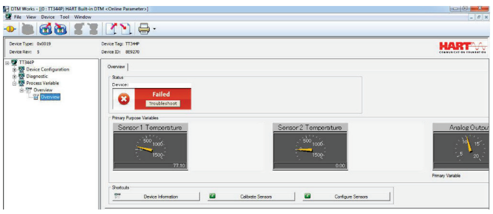

Figure 6. The main software interface

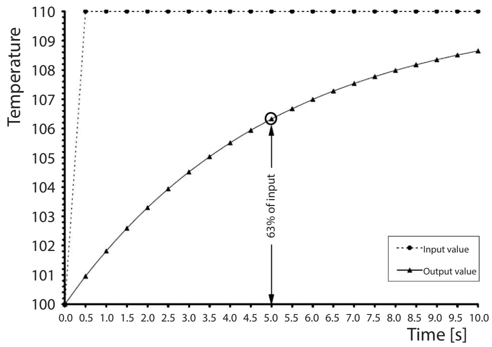

Figure 7. Temperature cloud map drawing interface

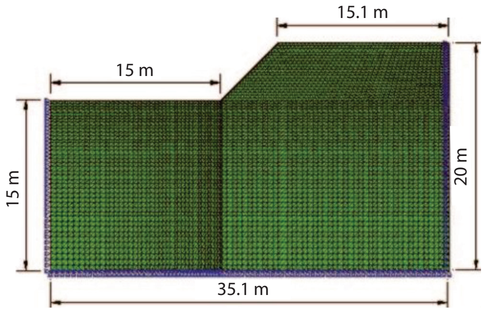

Figure 8. Finite element calculation model

Case analysis

Calculation model

A permafrost slope in the Osaka Mountain area of the Qinghai-Tibet Plateau, with a slope height of 5.0 m and a slope of 45°. The temperature change curve in this area is $T_a = -3 + 12\sin(2\pi t/8760 + \pi/2)$, the soil layer is a single homogeneous saturated clay, the physical parameters of the soil are shown in tab. 2, the dry density of the soil, ρ_d [kgm^{-3}], the initial water content, θ_0, the frozen soil unfrozen water content and the temperature relationship parameters a and b. Modulus of elasticity, Poisson-'s ratio and temperature relationship parameters a_1, b_1, a_2, b_2, and m, thawing coefficient A, thermal parameters are shown in tab. 3, melting soil heat capacity C_u [Jkg^{-1}°C^{-1}], thermal conductivity λ_u [Jkg^{-1}°C^{-1}], and water diffusion coefficient D_u [Jm^{-3}°C^{-1}], frozen soil heat capacity C_f [Jkg^{-1}°C^{-1}], thermal conductivity λ_f [Jm^{-1}°C^{-1}], and moisture. The finite element calculation model of diffusion coefficient D_f [Jm^{-3} °C^{-1}] is shown in fig. 8.

Table 2. Slope soil mechanical parameters

Physical quantity	ρ_d [kgm–3]	θ	a	b	a_1 [MPa]	b_1	a_2 [Mpa]	b_2	m	A
Value	1500	20%	9.982	0.435	8	18	0.3	0.02	0.6	0.6

Table 3. Thermal parameters of slope soil

Physical quantity	λ_u [Jm$^{–}$°C$^{–1}$]	C_u [Jkg$^{–1}$°C$^{–1}$]	λ_f [Jm$^{–1}$°C$^{–1}$]	C_f [Jkg$^{–1}$°C$^{–1}$]	D_u [Jm$^{–1}$°C$^{–1}$]	D_f [Jm$^{–1}$°C$^{–1}$]
Value	1.09	2.5092 · 106	1.22	$2.0701 \cdot 10^6$	$1.53 \cdot 10^{-8}$	$3.1 \cdot 10^{-11}$

Boundary conditions and initial conditions

Temperature boundary: According to the actual measurement results, the slope is $T_s = 0.7 + 13\sin(2\pi t/8760 + \pi/2)$, the toe and top of the slope are $T_s = -1.5 + 12\sin(2\pi t/8760 + \pi/2)$, the two sides are insulated, and the heat flux at the bottom is 0.06 W/m^2.

Water boundary: Does not consider water transpiration and infiltration exchange with the outside world [7].

Displacement boundary: Both sides are supported horizontally, the bottom side is horizontal and vertical support, and the other sides are free.

Solution process: Take the actual value of the frozen soil slope for the moisture content, then assign the initial value to the temperature, and combine the boundary to solve eqs. (4) and (2) to calculate the freeze-thaw cycle until the temperature and moisture below the seasonal active layer remain stable. At the same time, the value of each node is the same year by year, using the temperature and moisture of each node at this time as the initial value of the stability of the frozen soil layer, and then solving eqs. (7)-(9) to obtain the initial stress, and recalculating under the external seasonal freezing and thawing, Response of slope soil.

Result analysis

The slope goes through a freeze-thaw cycle, the freezing period (cold season) is from mid-October to mid-April of the following year (taken April 15th), and the thawing period (warm season is from mid-April to mid-October (taken October 15th). The end of the freezing period and the end of the thawing period are the two extreme states of the slope under the action of freezing and thawing. These two moments are selected for freezing and thawing analysis.

Analysis of slope temperature field under freezing and thawing

It can be seen from fig. 9 that the active layer of the slope changes alternately under the action of freezing and thawing, and the slope temperature field is significantly different at different times. At the end of freezing, the slope is completely frozen, and the thickness of the slope with greater negative temperature is thinner than the top and the toe of the slope [8]. At the end of melting, the melting thickness of the

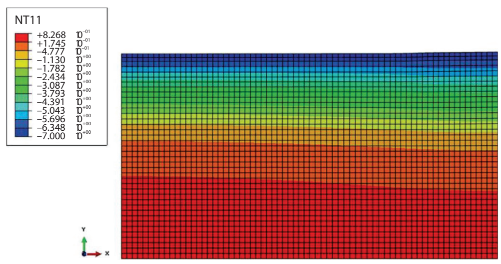

Figure 9. Slope temperature cloud map at different times

slope is larger than the top and toe of the slope. Freezing and thawing have a greater influence on the temperature of the slope, and thermal melting can cause the slope to slip, which is consistent with actual observations.

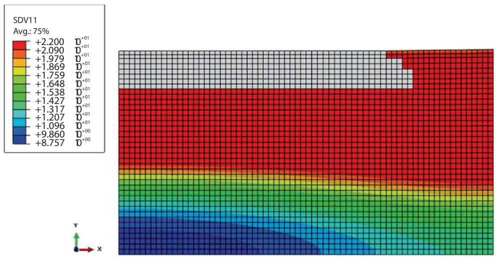

Figure 10. The unfrozen water content of the slope at different times

Analysis of slope moisture field under freezing and thawing

It can be seen from fig. 10 that at the end of the freezing period, the unfrozen water content of the active layer soil is lower than that of other parts. The unfrozen water content changes simultaneously with the temperature, and the size is determined by the temperature and the soil properties. At the end of thawing, the unfrozen water content of the active layer soil is significantly higher than that of other parts, and is the highest at the freeze-thaw interface, and the maximum water content is 20% greater than the initial water content [9]. At the end of the thawing period, the unfrozen water content is slightly greater than when it is frozen, indicating that water migration has occurred in the soil under the action of freezing and thawing, and the total water content has increased.

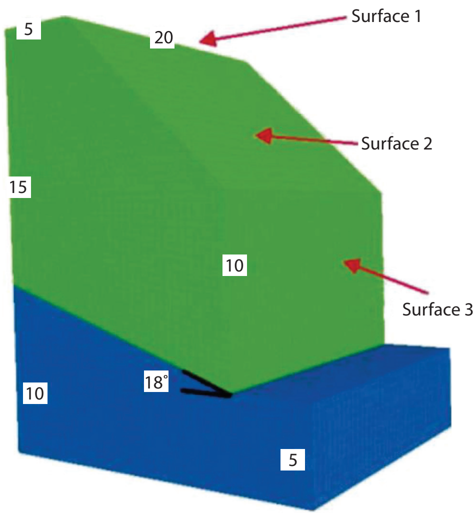

Figure 11. Cloud diagram of slope shear stress at different times

Analysis of slope shear stress under freeze-thaw action

It can be seen from fig. 11 that no matter when freezing or thawing is over, the shear stress near the freezing-thawing interface of the slope reaches the maximum and it is distributed in a band. The band is roughly parallel to the slope surface, but turning and small changes occur near the top and toe of the slope. The range extends without passing through the top and toe of the slope, and the shear stress of the rest is small and evenly distributed. The shear stress of the slope when freezing is greater than when melting [10]. The reason is that the soil below the upper limit of the slope is frozen and stable throughout the year, and the above soil is in a freeze-thaw alternate state, and moisture accumulates near the upper limit. Under the action of its own weight, the upper limit of the slope is the potential sliding surface of the frozen soil slope, so the shear stress is much greater than other parts. The elastic modulus of the soil during freezing is greater than that during melting, resulting in greater shear stress during freezing.

Analysis of slope horizontal displacement under freeze-thaw action

It can be seen from fig. 12 that at the end of the freezing period, the horizontal displacement of the slope is basically the same, the middle and lower parts are slightly larger, and the horizontal displacement is mainly caused by the frost heave of the soil. At the end of the thawing period, the horizontal displacement of the slope is small upwards and large downwards *protruding belly* shape. The top of the slope is affected by two-way freezing and thawing, and the top displacement is slightly larger than the displacement of the small area below the top. The horizontal displacement of the slope during freezing is much smaller than that during melting [11]. The reason is that during freezing (that is, in winter), the soil strength parameters increase, and a frozen soil skeleton is formed, mainly due to frost heave displacement, slope deformation is small, and stability good. During thermal thawing (that is, warm season) soil strength parameters decrease, unfrozen water content increases, slope stability under the action of dead weight and thermal thawing decreases, and slippage may occur, and warm-season thermal thawing should be emphasized in engineering design Instability.

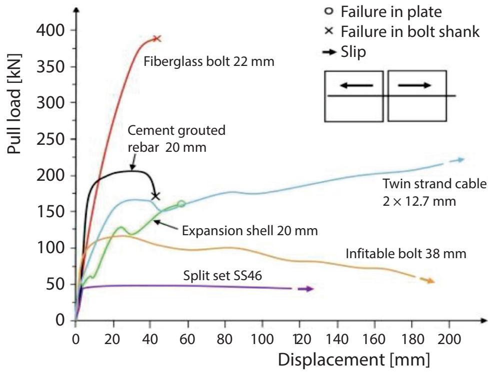

Figure 12. Horizontal displacement of the slope at different times

Conclusion

Based on the hydro-thermal-mechanical coupling theory and relying on MATLAB, a finite element program that can respond to the multi-field coupling mechanism of soil under freezing and thawing is compiled, and the reliability of the program is verified. Under the action of freezing and thawing, the active layer of the slope changes alternately between freezing and thawing. The temperature field of the frozen soil slope is significantly different at different times, and the maximum shear stress band appears at the freezing and thawing interface roughly parallel to the slope. At the end of the freezing period, the horizontal displacement of the slope is basically the same, with a slightly larger middle and lower part. At the end of the melting, the horizontal displacement of the slope is small upwards and large downwards, showing a *convex belly* shape. The unfrozen water content of the slope at the end of thawing, the horizontal displacement is greater than that of the frozen, and the maximum value of the shear stress is smaller than that of the frozen. The stability of permafrost in warm season is poor.

References

[1] Suo, Y., Liu, J., Thermo-Mechanical Coupling Analysis of a Cylindrical Lithium-Ion Battery with Thermal Radiation Effect in Generalized Plane Strain Condition, *International Journal of Energy Research*, *45* (2021), 2, pp. 1988-1998
[2] Rui, Y., Yin, M., Thermo-Hydro-Mechanical Coupling Analysis of a Thermo-Active Diaphragm Wall, *Canadian Geotechnical Journal*, *55* (2018), 5, pp. 720-735
[3] Rui, Y., Soga, K., Thermo-Hydro-Mechanical Coupling Analysis of a Thermal Pile, *Proceedings of the Institution of Civil Engineers-Geotechnical Engineering*, *172* (2019), 2, pp. 155-173
[4] Wu, S., Construction of Visual 3-D Fabric Reinforced Composite Thermal Perfomance Prediction System, *Thermal Science*, *23* (2019), 5, pp. 2857-2865
[5] Ye, W., *et al.*, Research on Thermo-Mechanical Coupling Deformation for the Ball Screw of Machine Tool Spindle Feed System, *Journal of Vibration Engineering & Technologies*, *8* (2020), 3, pp. 443-454
[6] Han, M. J., *et al.*, Low and High Cycle Fatigue of Automotive Brake Discs Using Coupled Thermo-Mechanical Finite Element Analysis under Thermal Loading, *Journal of Mechanical Science and Technology*, *32* (2018), 12, pp. 5777-5784
[7] Chen, G., *et al.*, Thermo-Mechanical Analysis of Friction Stir Welding: A Review on Recent Advances, (in English), *Acta Metallurgica Sinica*, *33* (2020), 1, pp. 3-12

[8] Wang, Y., *et al.*, Thermo-Mechanical Strong Coupling Analysis on Braking Device of Pipe Belt Conveyor, *Journal of Mechanical Science and Technology*, *32* (2018), 3, pp. 1277-1285
[9] Habib, F., *et al.*, Full Thermo-Mechanical Coupling Using Extended Finite Element Method in Quasi-Transient Crack Propagation, *Advanced Modelling and Simulation in Engineering Sciences*, *5* (2018), 18
[10] Wu, S., Study and Evaluation of Clustering Algorithm for Solubility and Thermodynamic Data of Glycerol Derivatives, *Thermal Science, 23* (2019), 5, pp. 2867-2875
[11] Oyanguren, A., *et al.*, Thermo-Mechanical Modelling of Ball Screw Preload Force Variation in Different Working Conditions, *The International Journal of Advanced Manufacturing Technology*, *97* (2018), 1, pp. 723-739

Paper submitted: December 26, 2020
Paper revised: January 30, 2021
Paper accepted: February 14, 2021